

# Validation of [ $^{18}\text{F}$ ]fluorodeoxyglucose and positron emission tomography (PET) for the measurement of intestinal metabolism in pigs, and evidence of intestinal insulin resistance in patients with morbid obesity

H. Honka · J. Mäkinen · J. C. Hannukainen ·  
M. Tarkia · V. Oikonen · M. Teräs · V. Fagerholm ·  
T. Ishizu · A. Saraste · C. Stark · T. Vähäsilta ·  
P. Salminen · A. Kirjavainen · M. Soinio · A. Gastaldelli ·  
J. Knuuti · P. Iozzo · P. Nuutila

Received: 9 November 2012 / Accepted: 17 December 2012 / Published online: 20 January 2013  
© Springer-Verlag Berlin Heidelberg 2013

## Abstract

**Aims/hypothesis** The role of the intestine in the pathogenesis of metabolic diseases is gaining much attention. We therefore sought to validate, using an animal model, the use of positron emission tomography (PET) in the estimation of intestinal glucose uptake (GU), and thereafter to test whether intestinal insulin-stimulated GU is altered in morbidly obese compared with healthy human participants.

**Methods** In the validation study, pigs were imaged using [ $^{18}\text{F}$ ]fluorodeoxyglucose ([ $^{18}\text{F}$ ]FDG) and the image-derived

data were compared with corresponding ex vivo measurements in tissue samples and with arterial–venous differences in glucose and [ $^{18}\text{F}$ ]FDG levels. In the clinical study, GU was measured in different regions of the intestine in lean ( $n=8$ ) and morbidly obese ( $n=8$ ) humans at baseline and during euglycaemic hyperinsulinaemia.

**Results** PET- and ex vivo-derived intestinal values were strongly correlated and most of the fluorine-18-derived radioactivity was accumulated in the mucosal layer of the gut wall. In the gut wall of pigs, insulin promoted GU as determined by PET, the arterial–venous balance or autoradiography. In lean human participants, insulin increased GU from the circulation in the duodenum (from  $1.3\pm 0.6$  to  $3.1\pm 1.1$   $\mu\text{mol}$  [ $100$  g] $^{-1}$  min $^{-1}$ ,  $p<0.05$ ) and in the jejunum (from  $1.1\pm 0.7$  to  $3.0\pm 1.5$   $\mu\text{mol}$  [ $100$  g] $^{-1}$  min $^{-1}$ ,  $p<0.05$ ). Obese participants failed to show any increase in insulin-stimulated GU compared with fasting values (NS).

**Conclusions/interpretation** Intestinal GU can be quantified in vivo by [ $^{18}\text{F}$ ]FDG PET. Intestinal insulin resistance occurs in obesity before the deterioration of systemic glucose tolerance.

**Electronic supplementary material** The online version of this article (doi:10.1007/s00125-012-2825-5) contains peer-reviewed but unedited supplementary material, which is available to authorised users.

H. Honka · J. Mäkinen · J. C. Hannukainen · M. Tarkia ·  
V. Oikonen · M. Teräs · V. Fagerholm · T. Ishizu · A. Saraste ·  
A. Kirjavainen · J. Knuuti · P. Nuutila (✉)  
Turku PET Centre, University of Turku, PL 52,  
FIN-20520 Turku, Finland  
e-mail: pirjo.nuutila@utu.fi

H. Honka · J. Mäkinen · A. Saraste · M. Soinio · P. Nuutila  
Department of Medicine, Turku University Hospital,  
Turku, Finland

C. Stark · T. Vähäsilta · P. Salminen  
Department of Surgery, Turku University Hospital, Turku, Finland

C. Stark · T. Vähäsilta  
The Research Centre of Applied and Preventive Cardiovascular  
Medicine, Medical Faculty, University of Turku, Turku, Finland

A. Gastaldelli · P. Iozzo  
Institute of Clinical Physiology, National Research Council,  
Pisa, Italy

**Keywords** Insulin action · Intermediary metabolism ·  
Molecular imaging

## Abbreviations

[ $^{18}\text{F}$ ]FDG	[ $^{18}\text{F}$ ]Fluorodeoxyglucose
FE	Fractional extraction
FUR	Fractional uptake rate
GU	Glucose uptake
HFD	High-fat diet
PET	Positron emission tomography

## Introduction

Evidence that the intestine plays a fundamental role in the pathogenesis of non-communicable diseases is rapidly accumulating. The intestine is a large organ and the first filter encountered by ingested substances. Moreover, it regulates nutrient absorption, secretes a number of potent hormones, controls local and systemic immunity, and interacts with the local microflora [1]. It has been shown that the endocrine function of the intestine deteriorates with ensuing type 2 diabetes [2]. The western diet is rich in fat and sugar, which contribute to the pathogenesis and progression of type 2 diabetes and associated illnesses. The effects of high plasma lipid and glucose levels on skeletal muscle, liver and pancreas are well documented [3], and primarily include insulin resistance and impaired beta cell function. In contrast, the effects of a high-fat diet (HFD) and hyperglycaemia on the metabolism of the small and large intestine are largely unknown.

Because most of the intestine is drained by the portal vein, the assessment of gut metabolism *in vivo* by arterial–venous measurements would be highly invasive and not practical in humans. Positron emission tomography (PET) is a standard imaging tool for cardiovascular, malignant and metabolic diseases. It relies on the use of radionuclide-labelled substrates and molecules. The assessment of tracer concentrations in the tissue of interest and in arterial plasma (input function) over time makes it possible to study the rate of clearance of the labelled molecule simultaneously at the whole-body and tissue-specific levels. [<sup>18</sup>F]Fluorodeoxyglucose ([<sup>18</sup>F]FDG) is the most widely used PET radiotracer for measurement of tissue glucose uptake (GU) [4–6]. To our knowledge, no validation study addressing the absolute quantification of gut metabolism by PET has been carried out.

The aims of this study were to quantify the effects of insulin on intestinal GU and to evaluate whether overnutrition and obesity lead to intestinal insulin resistance. To achieve these aims, a validation was carried out in pigs, including healthy and HFD-fed, streptozotocin-treated animals. GU in the duodenum, ileum and colon was measured *ex vivo* and *in vivo* by arterial–portal differences and by PET imaging in the fasting and insulin-stimulated states. The validated method was implemented in lean and morbidly obese humans during fasting and euglycaemic hyperinsulinaemia.

## Methods

**Animal study design** We studied 28 pigs (6 to 8 months old) in our animal protocols. Pigs were raised in the animal facility at Turku BioCity (Turku, Finland). The principles of laboratory animal care were followed and permission for

the study was obtained from the State Provincial Office of Southern Finland (ESAVI-2010-03970/Ym-23).

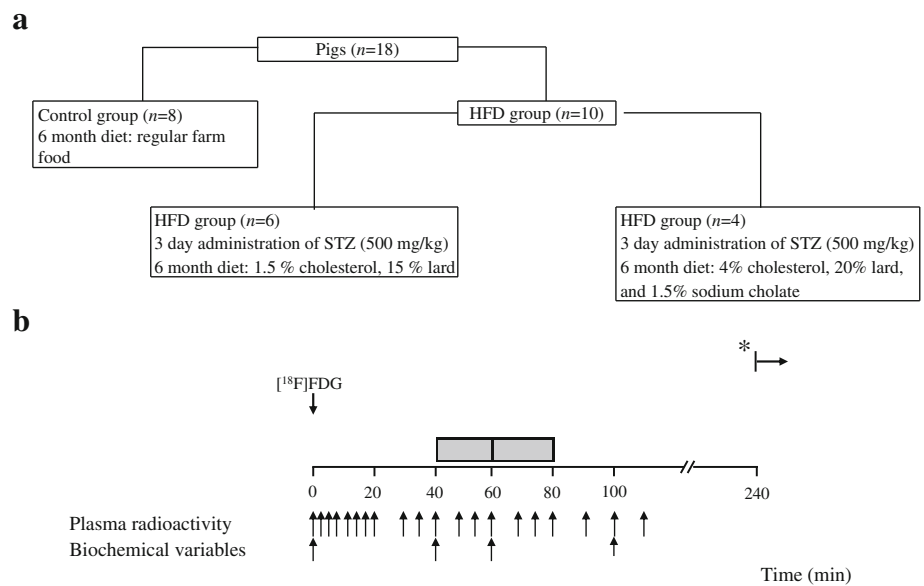
The dietary protocol included 18 pigs (Fig. 1), which were randomised into a control group ( $n=8$ ) and an HFD group ( $n=10$ ) in which hyperglycaemia and dyslipidaemia were induced by 3-day administration of streptozotocin (Zanosar, Pharmacia & Upjohn, MI, USA; 50 mg/kg in 0.1 mmol/l Na-citrate, pH4.5) and a 6-month HFD ( $n=6$ , 1.5% cholesterol and 15% lard;  $n=4$ , 4% cholesterol, 20% lard, 1.5% sodium cholate), respectively. PET imaging (hybrid PET/computed tomography scanner Discovery VCT; General Electric, Milwaukee, WI, USA) of the upper and lower abdomen was performed. One healthy pig of the dietary protocol was imaged during a euglycaemic–hyperinsulinaemic clamp to evaluate the effects of insulin. At the end of the imaging session, pigs were killed with intravenous potassium chloride to obtain intestinal tissue samples.

We studied ten pigs ( $n=6$  in the fasting state,  $n=4$  during euglycaemic hyperinsulinaemia) during co-administration of <sup>2</sup>H-labelled glucose and [<sup>18</sup>F]FDG, followed by frequent blood sampling to simultaneously measure the levels of <sup>2</sup>H-labelled glucose and [<sup>18</sup>F]FDG in the carotid artery and portal vein [7]. The ratio of the arterial–portal fractional extractions (FE) of the two compounds (defined as lumped constant) allows [<sup>18</sup>F]FDG data to be corrected for differences in glucose and [<sup>18</sup>F]FDG extraction by the intestine.

**Human study design** A total of eight morbidly obese individuals and eight age-matched lean control participants participated in the study. This study protocol is part of a larger human data collection (Sleevepass NCT00793143, <http://www.clinicaltrials.gov/ct2/show/NCT00793143>, last accessed May 2010) investigating the effects of bariatric surgery. Glucose tolerance was assessed by an OGTT. All participants underwent baseline PET imaging (Advance PET scanner; General Electric) during fasting and euglycaemic hyperinsulinaemia, as well as magnetic resonance imaging (Intera 1.5T; Philips, Best, the Netherlands). The protocol was repeated after bariatric surgery in the eight obese individuals. Bariatric surgery was clinically indicated in these patients. The Ethics Committee of the Hospital District of South Western Finland approved the study and all patients gave written informed consent before participation.

**Procedures and measurements in the animal study** After the induction of anaesthesia, peripheral venous catheters were placed in both ears, in the right carotid artery and in the portal vein of ten animals, as previously described [7]. Pigs were imaged in a supine position using a hybrid PET/computed tomography scanner (Discovery VCT; General Electric [8]). In the insulin clamp study, a prime-constant insulin infusion ( $1 \text{ mUkg}^{-1} \text{ min}^{-1}$ ) was started and euglycaemia was maintained by a variable glucose infusion. After the steady-

**Fig. 1** (a) Randomisation and (b) imaging protocol of the present animal study. Upright arrows indicate time point of determinations; grey shading indicates abdominal PET/CT; \* indicates laparotomy and ex vivo tissue sample collection; STZ, streptozotocin



state was reached (~45 min),  $[^{18}\text{F}]\text{FDG}$  was injected, followed by dynamic imaging. In fasting studies, saline was infused in place of insulin and glucose. An  $[^{18}\text{F}]\text{FDG}$  bolus ( $890 \pm 180$  MBq) was injected, followed by dynamic PET imaging of the upper and lower abdomen, starting 40 min after injection (20 min for each abdominal region). Arterial blood samples were collected to measure plasma  $[^{18}\text{F}]\text{FDG}$  concentrations over time, representing the amount of tracer that is available in the circulation for intestinal extraction (i.e. the input function). In ten animals,  $^2\text{H}$ -labelled glucose was co-injected with  $[^{18}\text{F}]\text{FDG}$  and portal vein blood samples were collected to measure tracer concentrations exiting the intestine. After the scanning, pigs were killed and tissue specimens from different intestinal parts obtained for ex vivo radioactivity analysis.

The intestinal lumped constant was determined as first described by Kelley et al [9], as the ratio between the FE of  $[^{18}\text{F}]\text{FDG}$  and  $^2\text{H}$ -labelled glucose. The FE were calculated as the cumulative sum of the arterial–portal concentration differences, normalised to the arterial concentrations, i.e.  $(a-v)/a$ , at each measurement time point [10, 11].

Ex vivo tissue  $[^{18}\text{F}]\text{FDG}$  radioactivity was measured using an automated gamma counter (Wizard 1480 3<sup>rd</sup>; Perkin-Elmer-Wallac, Turku, Finland) and normalised to the weight of the tissue specimen. The radioactivity measured in the tissue was divided by the area of the  $[^{18}\text{F}]\text{FDG}$  input function, representing the tracer that was available for intestinal extraction until tissue sampling. These results were compared with those obtained by PET imaging.

Histological preparations of tissue samples of duodenum, ileum and colon were stained and examined by autoradiography to quantify the distribution of  $[^{18}\text{F}]\text{FDG}$  between the mucosa and non-mucosa layers, in order to understand which layer of the intestine is responsive to insulin. The autoradiograms were analysed by densitometry using an

image software package (AIDA 4; Raytest, Straubenhardt, Germany). The mucosa and smooth muscle layer were outlined on the autoradiographic images and the ratio of mucosa:muscle signal intensity was calculated.

**Procedures and measurements in the human study** Human participants underwent PET imaging on two separate days, once in the fasting state and once during euglycaemic hyperinsulinaemia. Two catheters were inserted, one in a hand vein for the infusion of insulin and glucose, and the  $[^{18}\text{F}]\text{FDG}$  injection; the other catheter was inserted in the opposite antecubital arterialised vein for blood sampling. Human PET images were acquired in the supine position with an Advance PET scanner (General Electric [12]). A transmission scan of 5 min was performed to measure photon attenuation. After  $89 \pm 33$  min from the start of the euglycaemic–hyperinsulinaemic clamp or saline infusion (fasting studies),  $[^{18}\text{F}]\text{FDG}$  ( $191 \pm 9.1$  MBq) was injected and a dynamic scan of the upper abdominal region was performed, followed by a similar scan of the lower abdominal region. Arterialised blood samples were drawn to measure  $[^{18}\text{F}]\text{FDG}$  levels in plasma (input function). Anatomical reference was obtained using magnetic resonance images obtained using an Intera 1.5T scanner (Philips).

**Image processing and calculations** In animal and human protocols, raw data were corrected for tissue attenuation, dead time and decay, and reconstructed using standard algorithms in a  $256 \times 256$  matrix. Three-dimensional volumes of interest were manually drawn in duplicate into the duodenum, jejunum, ileum and colon (Carimas 2.0 software; Turku PET Centre, University of Turku, Turku, Finland) to obtain intestinal  $[^{18}\text{F}]\text{FDG}$  time–activity curves. Intestinal volumes of interest had a tubular shape to exclude spillover of radioactivity (i.e. contamination) from the contents of the

bowel. In human studies, the selection of volumes of interest was confirmed by manually co-registering magnetic resonance and PET images. The co-registration was evaluated visually in the gut and in other organs that are extremely well defined in PET images, such as the liver.

The rate constant for the transfer of [ $^{18}\text{F}$ ]FDG from plasma into the intestinal tissue was calculated from the time–activity curves in arterial plasma (input function), and in the duodenum, ileum and colon, using graphical analysis (Gjedde–Patlak plot) and the fractional uptake rate (FUR). These analyses have been extensively reported [4, 5] and are described in detail in the electronic supplementary material (ESM) text. In brief, the FUR represents the ratio of tissue [ $^{18}\text{F}$ ]FDG activity: integral of blood activity. The tissue measurement is obtained late after tracer injection, at a stage when an equilibrium is achieved, i.e. when plasma [ $^{18}\text{F}$ ]FDG levels entering the tissue are nearly constant, and the transfer rate can be reliably computed. Graphical analysis is based on the same principle, but uses several measurements of tissue activity in time to evaluate the transfer rate constant. In this case, data of tissue-to-plasma [ $^{18}\text{F}$ ]FDG activity over time are plotted as a function of the normalised cumulative integral of plasma [ $^{18}\text{F}$ ]FDG levels. Once an equilibrium is reached, the function becomes linear and its slope represents the transfer rate constant of [ $^{18}\text{F}$ ]FDG from

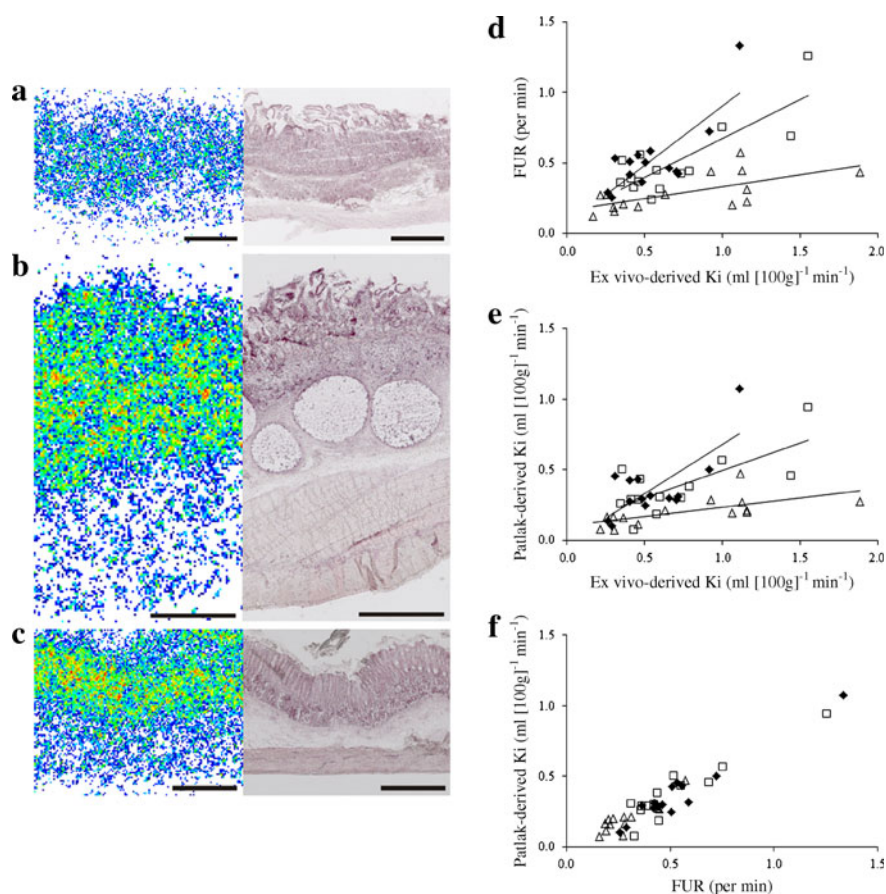
plasma into tissue; its intercept represents the initial tissue volume occupied by [ $^{18}\text{F}$ ]FDG ( $V_0$ ). See ESM text for further details.

The transfer rate constant of [ $^{18}\text{F}$ ]FDG was multiplied by plasma glucose levels and divided by the lumped constant to obtain rates of GU ( $\mu\text{mol min}^{-1}\text{g}^{-1}$ ). These data were compared with those obtained in tissue samples, as described above.

**Biochemical analyses** Arterial and plasma glucose levels were determined in duplicate by the glucose oxidase method (GM9 Analyser; AnaloX Instruments, London, UK). Plasma lactate was measured using a standard enzymatic method (Roche Molecular Biochemicals, Mannheim, Germany) with a fully automated analyser (Hitachi 704; Hitachi, Tokyo, Japan).

**Statistical analysis** Statistical analyses were performed using SAS software for Windows, version 9.2 (SAS Institute, Cary, NC, USA). Results are expressed as mean $\pm$ SD. Tests for equal variances and normality were performed. Where normal distribution was not apparent, median and ranges are presented. A simple  $t$  test was used to address differences between groups. Paired  $t$  tests were used to calculate differences within participants for validation purposes. The

**Fig. 2** Autoradiography analysis depicting  $^{18}\text{F}$ -derived radioactivity in (a) the duodenum, (b) the ileum and (c) the colon. Of the whole gut wall, 61%, 74% and 72% of [ $^{18}\text{F}$ ]FDG and therefore glucose accumulated in the mucosal layer of the respective sections of the gut wall. Scale bars 1 mm. Red/yellow colour indicates high tissue radioactivity, whereas green colour indicates intermediate and blue colour low tissue radioactivity, respectively. (d, e) Scatter plots showing differences between PET-derived in vivo data and ex vivo data calculated from tissue samples. Strong correlations were shown for all of the studied intestinal parts (black diamonds, duodenum; white squares, ileum; white triangles, colon). (f) The two different PET analysis methods (graphical analysis and FUR) were also strongly correlated. (d–f) all  $r$  values ranged between 0.63 and 0.97;  $p$  ranged from 0.02 to  $<0.0001$ .  $K_i$ , influx rate constant



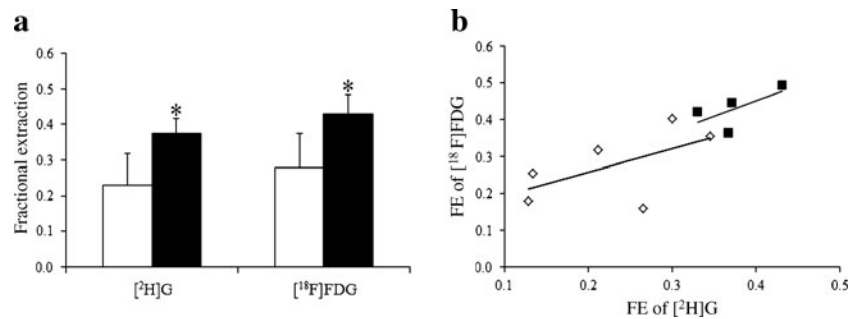


**Fig. 3** (a) Splanchnic FE of <sup>2</sup>H-labelled glucose ([<sup>2</sup>H]G) and [<sup>18</sup>F]FDG during fasting (white columns,  $n=6$ ) and euglycaemic hyperinsulinaemia (black columns,  $n=4$ ); \* $p<0.05$  vs corresponding fasting

values. (b) Insulin stimulation increased the FE of [<sup>18</sup>F]FDG and <sup>2</sup>H-labelled glucose. White symbols, fasting; black symbols, hyperinsulinaemia. Pooled data,  $r=0.80$ ,  $p<0.01$  (see *ESM* text)

Pearson correlation coefficient and significance of correlation were obtained wherever appropriate. A value of  $p<0.05$  was considered to be statistically significant.

## Results

**Validation in animal studies** Results obtained by graphical and FUR analyses were strongly correlated with each other and with ex vivo-derived results (Fig. 2d–f, *ESM* Figs 1 and 2). Absolute values of intestinal [<sup>18</sup>F]FDG transfer rate constants and of GU, as obtained with FUR, were similar to the ones obtained by ex vivo measurements. Both were higher than the estimations derived by graphical analysis. The arterial–portal differences for [<sup>18</sup>F]FDG and <sup>2</sup>H-labelled glucose were significantly correlated (Fig. 3a), with ratios (lumped constants) of 1.30 and 1.15 during fasting and hyperinsulinaemia, respectively, documenting that the intestinal FE of [<sup>18</sup>F]FDG is slightly superior to that of glucose (Fig. 3b). Autoradiography analysis and subsequent histological staining of intestinal tissue sections showed that most of the <sup>18</sup>F was located in the mucosal layer of the intestinal wall, compared with significantly lower levels in the non-mucosal layer (i.e. submucosa, muscularis propriae and serosa) (Fig. 2a–c). For further details, see *ESM* text.

**Intestinal glucose metabolism in animal studies** The HFD led to a significant deterioration of plasma glucose and cholesterol levels, HDL:cholesterol ratio and mean blood pressure in HFD vs control animals (Table 1). Insulin levels were below the detection limit (1.4 pmol/l) in all pigs. In the HFD group, only one pig did not have fasting hyperglycaemia (fasting plasma glucose 6.3 mmol/l). Fasting duodenal GU, as measured in ex vivo tissue samples, was significantly greater in the HFD than in the control group (*ESM* Figs 1 and 2). In the HFD group, fasting plasma glucose levels were correlated with GU in the duodenum and ileum, but not with that in the colon ( $r=0.65$ ,  $p<0.05$ ;  $r=0.52$ ,  $p=0.03$ ;

$r=-0.26$ , NS, respectively). For comparison, fasting GU data were calculated in the liver and skeletal muscle, showing that intestinal GU values ( $3.7\pm 1.5$ ,  $5.1\pm 2.5$  and  $4.1\pm 2.2$   $\mu\text{mol [100 g]}^{-1}\text{min}^{-1}$  for duodenum, ileum and colon, respectively) were in the same order of magnitude and closer to hepatic ( $3.2\pm 2.0$   $\mu\text{mol [100 g]}^{-1}\text{min}^{-1}$ ) than to muscle ( $0.71\pm 0.47$   $\mu\text{mol [100 g]}^{-1}\text{min}^{-1}$ ) GU values. Intestinal GU values in the pig studied during hyperinsulinaemia were markedly higher than fasting GU data in the duodenum, ileum and colon (*ESM* Table 1). This result was confirmed in the autoradiography analysis (insulin-stimulated vs fasting state, ratios: 1.9 vs 1.7, 3.7 vs 3.4, 3.7 vs 2.9 in the duodenum, ileum and colon, respectively). Moreover, arterial–portal differences in FE of [<sup>18</sup>F]FDG and <sup>2</sup>H-labelled glucose were markedly increased in response to insulin stimulation (Fig. 3a).

**Intestinal glucose metabolism in human studies** Obese patients had normal glucose tolerance, as assessed by the 2 h glycaemic value during the OGTT (range 5.0–7.3 mmol/l and 5.0–7.6 mmol/l in patients and controls, respectively, NS) (Table 2). Insulin-mediated whole-body GU was markedly reduced in obese patients compared with controls

**Table 1** Metabolic and biochemical characteristics in control and HFD pigs aged 6 to 8 months

Characteristic	Control group $n=8$	HFD group $n=10$	$p$ value
Weight (kg)	82±9.7	126±7.6	<0.0001
Mean arterial pressure (mmHg)	82±15	106±21	0.02
Glucose (mmol/l)	6.0±2.2	12±5.0	0.004
Cholesterol (mmol/l)	2.0±0.3	12±3.5	<0.0001
HDL-cholesterol (%)	56±6.5	29±6.4	<0.0001
Triacylglycerol (mmol/l)	1.4±0.8	1.5±0.9	0.52
Lactate (mmol/l)	1.2±0.8	0.9±0.4	0.42

Values are mean±SD

**Table 2** Anthropometric and metabolic characteristics of human participants

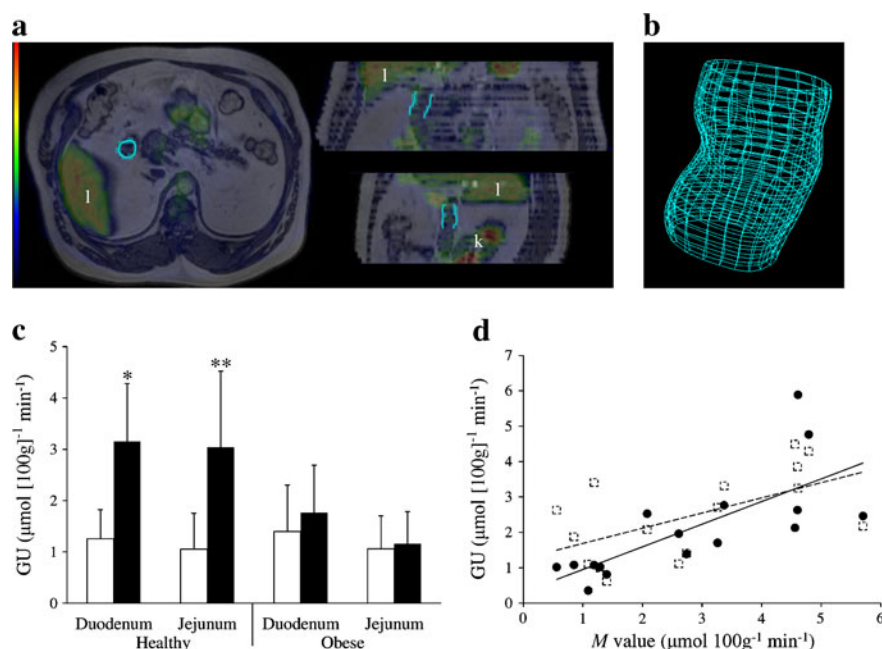
Characteristic <i>n</i>	Healthy 8	Obese 8	<i>p</i> value
Age (years)	45.9±5.8	40.8±8.1	0.17
Women ( <i>n</i> )	2	8	
Men ( <i>n</i> )	6	0	
Weight (kg)	70.3±7.1	118.4±12.8	<0.0001
BMI (kg/m <sup>2</sup> )	24.0±1.85	43.9±4.1	<0.0001
Fasting glucose (mmol/l)	5.3±0.4	5.4±0.5	0.78
HbA <sub>1c</sub> (%)	5.7±0.2	5.5±0.3	0.3
HbA <sub>1c</sub> (mmol/mol)	38.9±2.5	36.6±3.6	0.2
2 h Glucose in OGTT (mmol/l)	5.8±1.3	6.0±0.9	0.69
<i>M</i> value (μmol kg <sup>-1</sup> min <sup>-1</sup> )	41.9±10.1	14.0±7.0	<0.0001

Values are mean±SD

*M* value, whole-body glucose disposal

(Table 2). In healthy volunteers, hyperinsulinaemia increased GU in the duodenum ( $1.3\pm 0.6$  vs  $3.1\pm 1.1$  μmol [100 g]<sup>-1</sup> min<sup>-1</sup>,  $p<0.05$ ) and in the jejunum ( $1.1\pm 0.7$  vs  $3.0\pm 1.5$  μmol [100 g]<sup>-1</sup> min<sup>-1</sup>,  $p<0.05$ ) (Fig. 4c) by two- to threefold over fasting values. Compared with healthy volunteers, obese patients showed similar intestinal GU in the fasting state. As opposed to lean controls, no significant response to insulin was observed in morbidly obese patients (Fig. 4c). In the pooled groups, a significant positive correlation was found between insulin-stimulated intestinal GU and whole-body GU (*M* value) (Fig. 4d).

**Fig. 4** (a) Transaxial, coronal and sagittal projections of (b) a duodenal volume of interest in an obese human participant. Care was taken to avoid intestinal contents and surrounding tissues, such as the liver (l) and kidneys (k). (c) GU in the duodenum and jejunum during fasting (white columns) and euglycaemic–hyperinsulinaemic clamp (black columns) in lean controls and obese participants; \* $p<0.05$  and \*\* $p<0.01$  vs corresponding fasting values. (d) GU in the duodenum (white circles) and jejunum (black squares) correlated positively with whole-body GU (*M* value). The data include healthy and obese groups;  $r=0.58$ ,  $p<0.05$  and  $r=0.73$ ,  $p<0.005$ , respectively



## Discussion

This study demonstrates that PET represents a novel tool for the investigation of gut metabolism, its alterations and interaction with substrates and hormones in humans in vivo. It also shows that obesity leads to intestinal insulin resistance in animals and humans.

GU rates derived from ex vivo tissue samples correlated strongly with the values calculated using common PET data analysis methods. The lumped constant, which defines the ratio of [<sup>18</sup>F]FDG:glucose in relation to transmembrane transport and hexokinase-mediated phosphorylation [10, 11], was found to be 1.30 and 1.15 during fasting and hyperinsulinaemia, respectively. These figures are very similar to those reported in the liver [7], skeletal muscle [13] and adipose tissue [14]. Due to the limited resolution, PET images cannot differentiate the relative distribution of [<sup>18</sup>F]FDG in different intestinal layers. Therefore, the biodistribution of [<sup>18</sup>F]FDG was examined by autoradiography in the mucosa and muscle layers. We found that a majority of <sup>18</sup>F-derived intestinal radioactivity was located in the mucosal layer during the fasting state and during hyperinsulinaemic euglycaemia. Altogether, the findings of the study support the use of PET for the assessment of intestinal glucose metabolism.

In pigs, ex vivo-derived duodenal GU values were found to be significantly higher [15], while colonic GU values tended to be lower in the HFD than in the control group (ESM Fig. 1). However, the diversified metabolism in different bowel tracts may not have been fully captured by the PET and ex vivo analysis methods adopted in this study, which address only the irreversible proportion of GU. In

most organs, this would correspond to the total amount of glucose entering the cells and being phosphorylated. However, as the gut is a gluconeogenic organ, glucose- or [ $^{18}\text{F}$ ]FDG-6-phosphate can be dephosphorylated and released back into the circulation. Although [16] the gut accounts for a small percentage of whole-body glucose production during the first 12 to 24 h of fasting, reaching values of 20% after 48 h in rats, it is of interest that levels of the enzymes involved in gluconeogenesis (phosphoenolpyruvate carboxykinase and glucose-6-phosphatase) are different in the proximal vs the distal small intestine [17–21]. Enzymatic differences might be one reason why the uptake of glucose was increased in the duodenum and not in the colon in HFD compared with healthy pigs.

The most important findings of our study relate to the evidence that the intestine is highly responsive to insulin in animals and humans. Intestinal FE of [ $^{18}\text{F}$ ]FDG and  $^2\text{H}$ -labelled glucose were found to be augmented by more than 50% during insulin stimulation. Moreover, tissue autoradiography showed that the majority of [ $^{18}\text{F}$ ]FDG was localised in the mucosal layer, with higher intensity ratios in the insulin-stimulated experiment than during the fasting state in all parts of the intestine. Previous studies have shown that GU in the small intestine of dogs is increased during combined hyperinsulinaemia and hyperglycaemia [22], and that gluconeogenesis in the small intestine of rats is blunted by insulin infusion [18]. Conversely, Barrett et al [22] did not observe a significant increase in extra-hepatic splanchnic GU during euglycaemic hyperinsulinaemia in dogs. However, a tendency towards an increase can be observed in their data, which may have failed to achieve significance due to the assessment of net (rather than unidirectional) GU values. In addition, we cannot rule out species-related differences. We used independent approaches to estimate the influx of glucose in the intestine, namely the arterial–venous balance of  $^2\text{H}$ -labelled glucose and of [ $^{18}\text{F}$ ]FDG. Together with PET imaging, these approaches were consistent in supporting the notion that insulin promotes intestinal GU in the pig, a finding we confirmed in healthy humans. Our data thus seem to conclusively demonstrate that the intestinal mucosa is an insulin-sensitive organ, at least in pigs and humans.

When healthy human volunteers were studied during fasting and insulin stimulation, we found that insulin was able to increase GU by 2.5- and 2.9-fold in the duodenum and jejunum, respectively. The most salient observation in our human study was that, compared with healthy individuals, our obese non-diabetic participants had similar intestinal GU in the fasting state, but showed no response to insulin, implying insulin insensitivity of the small intestine. Two considerations are important here. First, since the intestine represents a large organ in the body, the severe impairment of intestinal GU observed here may significantly affect systemic glucose metabolism. In fact, our data indicate that intestinal GU was

similar to liver GU and greater than skeletal muscle GU in pigs. Both humans and pigs have 0.1 m of intestine per kg body weight; the intestine, moreover, is the heaviest internal organ in the body, weighing approximately 3 to 4 kg. Second, as the obese participants were still normally glucose-tolerant, intestinal insulin resistance seems to precede type 2 diabetes. Our study was designed to explore the effects of insulin and obesity on intestinal metabolism, but we did not address the molecular mechanisms explaining intestinal insulin resistance in relation to obesity. A lack of suppression of gluconeogenesis or impaired stimulation of glucose transport and metabolism by insulin may both be involved. The production of gluconeogenic enzymes is strongly inhibited by insulin in the intestinal mucosa, affecting basolateral GU [16]. However, after a 12 h fasting period, intestinal gluconeogenesis is not very active. Thus, studies addressing the insulin signalling and glucose transport pathways [17, 23, 24] are required.

What are the clinical implications of our methodological developments and results? Abnormalities in intestinal glucose metabolism are likely to be present in several diseases, including inflammatory bowel diseases, obesity and diabetes. Our main objectives are to understand the molecular causes of such abnormalities, and to evaluate whether the gut microflora may be responsible for intestinal insulin resistance and if the latter can lead to impaired release of gastrointestinal hormones. These questions address aspects of pathophysiology and the identification of drug targets. As demonstrated in the skeletal muscle, liver, heart, adipose tissue and brain [7, 11, 15, 25–27], PET can be a useful tool to demonstrate drug efficacy, once glucose metabolism is altered at the level of specific organs. However, due to the cost, complexity and use of radioactive tracers, large-scale screening of patients for diagnostic purposes is not among the realistic perspectives of this technology.

In conclusion, intestinal [ $^{18}\text{F}$ ]FDG PET is a reliable method for the estimation of intestinal GU. Our animal and human data provide evidence of insulin sensitivity in the mucosal layer of the intestine, and of intestinal insulin resistance in obese non-diabetic human participants. The occurrence of mucosal insulin resistance in the early stages of the metabolic syndrome may partly be a cause or an effect of the typical changes in intestinal function observed in these illnesses, most notably altered incretin production [2], metabolic endotoxaemia [28] and gut  $\times$  bacterial interaction [29]. Further studies are warranted to clarify the relevance and consequences of intestinal insulin resistance, and the possibility of preventing or reversing it.

**Acknowledgements** The authors thank the staff of the Turku PET Centre for performing PET imaging and laboratory analyses. We also thank I. Lisinen (Department of Medicine, Turku University Hospital, Turku, Finland) for her statistical expertise. The study was conducted within the Finnish Centre of Excellence in Molecular Imaging in Cardiovascular and Metabolic Research.

**Funding** This study was supported by the Academy of Finland, University of Turku, Turku University Hospital, Åbo Akademi University, and by TEKES, Finnish Diabetes Foundation and Sigrid Juselius Foundation.

**Duality of interest** The authors declare that there is no duality of interest associated with this manuscript.

**Contribution statement** HH, JM: acquisition of data, analysis and interpretation of data, drafting of the manuscript, statistical analysis. JCH: acquisition of data, analysis and interpretation of data, critical revision of the manuscript for important intellectual content, study supervision. MT, AG: acquisition of data, analysis and interpretation of data, critical revision of the manuscript for important intellectual content. VO: analysis and interpretation of data, and critical revision of the manuscript for important intellectual content. MT: analysis and interpretation of data, critical revision of the manuscript for important intellectual content, technical support. VF, TI, CS, TV, PS, AK, MS: acquisition of data and critical revision of the manuscript for important intellectual content. AS: conception and design, acquisition of data, critical revision of the manuscript for important intellectual content. JK: conception and design, critical revision of the manuscript for important intellectual content, administrative support. PI: analysis and interpretation of data, critical revision of the manuscript for important intellectual content, study supervision. PN: design and supervision of the human study, analysis and interpretation of data, critical revision of the manuscript for important intellectual content, study supervision. All authors approved the final version of manuscript.

## References

- Delzenne N, Neyrinck A, Bäckhed F et al (2011) Targeting gut microbiota in obesity: effects of prebiotics and probiotics. *Nat Rev Endocrinol* 7:639–646
- Holst JJ, Vilsboll T, Deacon CF (2009) The incretin system and its role in type 2 diabetes mellitus. *Mol Cell Endocrinol* 297:127–136
- Lin Y, Sun Z (2010) Current views on type 2 diabetes. *J Endocrinol* 204:1–11
- Patlak CS, Blasberg RG, Fenstermacher JD (1983) Graphical evaluation of blood-to-brain transfer constants from multiple-time uptake data. *J Cereb Blood Flow Metab* 3:1–7
- Ishizu K, Nishizawa S, Yonekura Y et al (1994) Effects of hyperglycemia on FDG uptake in human brain and glioma. *J Nucl Med* 35:1104–1109
- Thie JA (1995) Clarification of a fractional uptake concept. *J Nucl Med* 36:711–712
- Iozzo P, Jarvisalo MJ, Kiss J et al (2007) Quantification of liver glucose metabolism by positron emission tomography: validation study in pigs. *Gastroenterology* 132:531–542
- Teras M, Tolvanen T, Johansson JJ, Williams JJ, Knuuti J (2007) Performance of the new generation of whole-body PET/CT scanners: discovery STE and Discovery VCT. *Eur J Nucl Med Mol Imaging* 34:1683–1692
- Kelley DE, Williams KV, Price JC, Goodpaster B (1999) Determination of the lumped constant for [<sup>18</sup>F] fluorodeoxyglucose in human skeletal muscle. *J Nucl Med* 40:1798–1804
- Crane PD, Pardridge WM, Braun LD, Oldendorf WH (1983) Kinetics of transport and phosphorylation of 2-fluoro-2-deoxy-D-glucose in rat brain. *J Neurochem* 40:160–167
- Bessell EM, Foster AB, Westwood JH (1972) The use of deoxyfluoro-D-glucopyranoses and related compounds in a study of yeast hexokinase specificity. *Biochem J* 128:199–204
- DeGrado TR, Turkington TG, Williams JJ, Stearns CW, Hoffman JM, Coleman RE (1994) Performance characteristics of a whole-body PET scanner. *J Nucl Med* 35:1398–1406
- Haaparanta M, Paul R, Gronroos T, Bergman J, Kamarainen EL, Solin O (2003) Microdialysis and 2-[<sup>18</sup>F]fluoro-2-deoxy-D-glucose (FDG): a study on insulin action on FDG transport, uptake and metabolism in rat muscle, liver and adipose tissue. *Life Sci* 73:1437–1451
- Virtanen KA, Peltoniemi P, Marjamaki P et al (2001) Human adipose tissue glucose uptake determined using [(18)F]-fluoro-deoxy-glucose ([<sup>18</sup>F]FDG) and PET in combination with microdialysis. *Diabetologia* 44:2171–2179
- del Prato S, Matsuda M, Simonson DC et al (1997) Studies on the mass action effect of glucose in NIDDM and IDDM: evidence for glucose resistance. *Diabetologia* 40:687–697
- Mithieux G (2001) New data and concepts on glutamine and glucose metabolism in the gut. *Curr Opin Clin Nutr Metab Care* 4:267–271
- Mithieux G (2012) A synergy between incretin effect and intestinal gluconeogenesis accounting for the rapid metabolic benefits of gastric bypass surgery. *Curr Diab Rep* 12:167–171
- Croset M, Rajas F, Zitoun C et al (2001) Rat small intestine is an insulin-sensitive gluconeogenic organ. *Diabetes* 50:740–746
- Rajas F, Bruni N, Montano S et al (1999) The glucose-6 phosphatase gene is expressed in human and rat small intestine: regulation of expression in fasted and diabetic rats. *Gastroenterology* 117:132–139
- Mithieux G, Bady I, Gautier A et al (2003) Induction of control genes in intestinal gluconeogenesis is sequential during fasting and maximal in diabetes. *Am J Physiol Endocrinol Metab* 286:370–375
- Mithieux G, Rajas F, Gautier-Stein A (2004) A novel role for glucose 6-phosphatase in the small intestine in the control of glucose homeostasis. *J Biol Chem* 279:44231–44234
- Barrett EJ, Ferrannini E, Gusberg R, Bevilacqua S, DeFronzo RA (1985) Hepatic and extrahepatic splanchnic glucose metabolism in the postabsorptive and glucose fed dog. *Metabolism* 34:410–420
- Tobin V, Le Gall M, Fioramonti X et al (2008) Insulin internalizes GLUT2 in the enterocytes of healthy but not insulin-resistant mice. *Diabetes* 57:555–562
- Ait-Omar A, Monteiro-Sepulveda M, Poitou C et al (2011) GLUT2 accumulation in enterocyte apical and intracellular membranes: a study in morbidly obese human subjects and ob/ob and high fat-fed mice. *Diabetes* 60:2598–2607
- Gontier E, Fourme E, Wartski M et al (2008) High and typical <sup>18</sup>F-FDG bowel uptake in patients treated with metformin. *Eur J Nucl Med Mol Imaging* 35:95–99
- Saraste A, Nekolla S, Schwaiger M (2009) Cardiovascular molecular imaging: an overview. *Cardiovasc Res* 83:643–652
- Rinne J (1999) Drug development for neurodegenerative diseases: role of PET. *Ann Med* 31:444–449
- Pendyala S, Walker JM, Holt PR (2012) A high-fat diet is associated with endotoxemia that originates from the gut. *Gastroenterology* 142:1100–1101.e2
- Ding S, Chi MM, Scull BP et al (2010) High-fat diet: bacteria interactions promote intestinal inflammation which precedes and correlates with obesity and insulin resistance in mouse. *PLoS One* 5:e12191